

dam, 1969), p. 655; A. Temkin, A. K. Bhatia, and E. Sullivan, *Phys. Rev.* **176**, 80 (1968). The dipole normalization factor was first derived in this last reference with an omission corrected in A. Temkin and Y. Hahn, *Phys. Rev. A* **10**, 708 (1974).

<sup>2</sup>Temkin and Hahn, Ref. 1.

<sup>3</sup>A. Temkin, *J. Phys. B* **7**, L450 (1974).

<sup>4</sup>A. Temkin, in *Proceedings of the Study Weekend on Collision Processes*, Daresbury Laboratory, 26-27 March 1982 (to be published).

<sup>5</sup>J. B. Donahue, P. A. M. Gram, H. V. Hynes, R. W. Hamm, C. A. Frost, H. C. Bryant, K. B. Butterfield, D. A. Clark, and W. W. Smith, *Phys. Rev. Lett.* **48**, 1538 (1982).

<sup>6</sup>G. H. Wannier, *Phys. Rev.* **90**, 817 (1953).

<sup>7</sup>R. Peterkop, *J. Phys. B* **4**, 513 (1971).

<sup>8</sup>A. R. P. Rau, *Phys. Rev. A* **4**, 207 (1971).

<sup>9</sup>A. Temkin, *Comments At. Mol. Phys.* **11**, 287 (1982).

<sup>10</sup>C. Bottcher, *J. Phys. B* **14**, L349 (1981).

<sup>11</sup>C. Bottcher, to be published.

<sup>12</sup>S. Cvejanovic and F. H. Read, *J. Phys. B* **7**, 1841 (1974).

<sup>13</sup>Cf. W. C. Lineberger, H. Hotop, and T. A. Patterson, in *Electron and Photon Interactions with Atoms*, edited by H. Kleinpoppen and M. R. C. McDowell (Plenum, New York, 1976), p. 125.

<sup>14</sup>A. Temkin, *J. Phys. B* **15**, L301 (1982).

<sup>15</sup>H. Klar, *J. Phys. B* **14**, 4165 (1981).

## Fractional Mode Numbers in Wavy Taylor Vortex Flow

Guenter Ahlers, David S. Cannell, and M. A. Dominguez Lerma

*Department of Physics, University of California, Santa Barbara, California 93106*

(Received 3 May 1982)

Spectral power and phase measurements are presented which demonstrate the existence of a wavy Taylor vortex-flow state with a mode number  $m = \frac{3}{2}$ . The mode is periodically continued around the annulus by a phase anomaly which is stationary in the laboratory frame. It is also shown that wavy Taylor vortex flow results in an increase (decrease) of the Taylor vortex-pair width near the center (ends) of the apparatus.

PACS numbers: 47.20.+m, 47.35.+i

Fluid flow experiments often reveal that boundary conditions result in spatially periodic velocity fields with an integer number of wavelengths filling the container. The most extensive example is perhaps based on the study by Coles<sup>1</sup> of the Couette-Taylor system of a fluid contained between two concentric cylinders with the inner one rotating. In that case, the flow could be described by the (integer) number  $p$  of Taylor vortices filling the system in the axial direction and the (integer) number  $m$  of wavelengths of a wavy mode traveling azimuthally. We report in this Letter measurements on a wavy Taylor vortex-flow (WVF) mode with *non*integer mode number  $m = \frac{3}{2}$ . The existence of fractional mode numbers should be of importance in classifying the various routes to nonperiodic, or turbulent, flow. The classification of WVF states and of modulated wavy vortex-flow (MWVF) states by Gorman, Swinney, and Rand<sup>2</sup> and by Rand<sup>3</sup> does not include low-symmetry modes such as ours.

Our apparatus consists of two concentric cylinders, with the inner one rotating and the outer one stationary. The inner radius was  $r_i = 3.118$

cm, and the radius ratio  $\eta \equiv r_i/r_o$  was 0.893. The upper and lower boundaries were rigid and non-rotating. We studied the aspect ratio  $L \equiv H/d = 53.9$  ( $H$  = column height and  $d = r_o - r_i$ ). The temperature was constant and uniform to  $\pm 5 \times 10^{-3}$  °C, and the cylinder speed was controlled accurately by a frequency synthesizer. The fluid was a 30% solution of glycerol in water by volume, with 0.6% by volume of a "Kalliroscope" suspension added for flow visualization. Two independent light reflectance probes were used to study the time dependence of the visualized flow. Each probe consisted of a normally incident 2-mW He-Ne laser beam and a photovoltaic detector. The signals were sampled simultaneously and both probes could be translated vertically with a resolution of 13  $\mu$ m.

Upon increase of the angular speed  $\Omega$  of the inner cylinder, and thus the Reynolds number  $R$ , a transition occurred at  $R \equiv R_c$  from azimuthal flow (except near the ends) to a primary-mode<sup>4</sup> Taylor vortex-flow (TVF) state consisting of toroidal vortices with an axial wavelength  $\lambda \approx 2.0$ . (All lengths will be reduced by the gap  $d$ .) For

$R > R_c$ , we find that  $\lambda$  can be varied continuously, maintaining an even  $p$ , over a range (which depends upon  $R$ ) by changing  $L$ . For fixed  $L$ ,  $\lambda$  can be changed in discrete steps by changing  $p$ . For  $R > R_w > R_c$ , azimuthal traveling waves appear on the vortices.  $R_w$  depends upon  $\lambda$  and, for our geometry,  $R_w/R_c = 1.13$  for  $\lambda = 1.8$ , 1.12 for  $\lambda = 2.0$ , and 1.16 for  $\lambda = 2.45$ . If  $R$  is increased quasistatically beyond  $R_w$ , we always find that a WVF state is formed which has three waves around the circumference of the cylinder, corresponding to a mode number  $m = 3$ . In the WVF state, the power spectrum of the photovoltaic signal consists of instrumentally sharp lines at integer multiples of the frequency  $\omega_1 = m\Omega s$ , where  $s \approx 0.46$  is the dimensionless speed of the wave. Although  $s$  varies by only a few percent, it does depend upon  $\lambda$ ,  $m$ , and  $R$ . Many of the above observations have also been reported by others.<sup>5</sup>

For our  $L = 53.9$ , we can create TVF states with  $p = 58, 56, \dots, 42$  for  $R$  close to but less than  $R_w$ . Quasistatic increases in  $R$  then yield  $m = 3$ . However, for larger  $R$ , all WVF states with  $p \neq 46$  eventually become unstable and decay to states with larger or smaller  $p$  and  $m = 3$ , until only  $p = 46$ ,  $m = 3$  survives for  $R$  near  $1.45R_c$ .<sup>6</sup> Near  $R_{1/2} = 1.50R_c$ , the spectral features of this state are changed dramatically by the appearance of a strong subharmonic. The new frequency is equal to  $\omega_1/2$  within 2 parts in  $10^4$ . The new spectral line is also instrumentally sharp. At the subharmonic bifurcation, there is no noticeable singularity in the speed of the  $m = 3$  mode. Upon further increase of  $R$ , a quasiperiodic state is entered with the subharmonic and the fundamental frequency  $\omega_1$  remaining prominent.

If the speed of the subharmonic is the same as that of the  $m = 3$  mode, then it has the mode number  $m = \frac{3}{2}$ . Since such a mode would not be periodic around the annulus, an anomaly in the phase would have to exist. Alternatively, the speed of this mode could be less by a factor of 2, and the mode number  $m = 3$  could be retained. In order to explore the symmetry of the subharmonic, we made spectral power measurements at the frequencies  $\omega_1/2$ ,  $\omega_1$ , and  $2\omega_1$  as a function of distance  $l$  above the lower boundary. Examples of the power measurements are shown in Fig. 1. They are based on over fifty 2048-point time series, taken one each at successive vertical positions near the column center and separated by  $\Delta l \approx 0.1$ . The power at  $\omega_1/2$  and at  $2\omega_1$  is highly concentrated in two peaks located near the mean positions of outflow vortex boundaries and sepa-

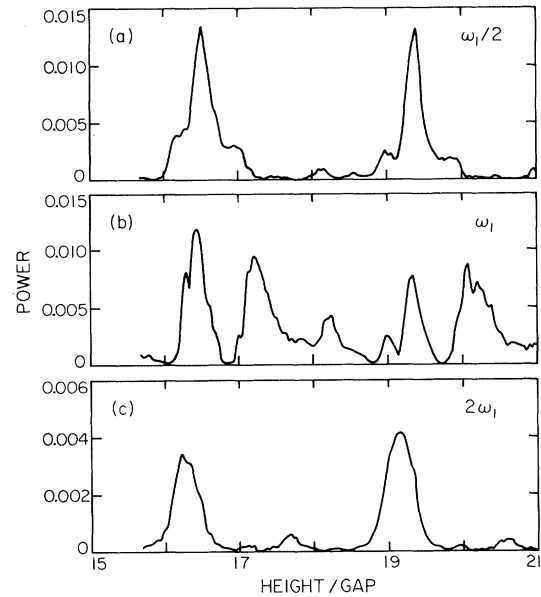


FIG. 1. Spectral power, in arbitrary units, at three frequencies, as a function of distance above the bottom end of the column and for  $R/R_c = 1.503$ .

rated by one TVF wavelength. The power at  $\omega_1$  has a more complicated structure, but measurements over a wide range of  $l$  show that it also repeats approximately with the TVF periodicity. The results show that the *power* of the new mode has the same axial periodicity as the  $m = 3$  mode and the vortex pairs, but of course they yield no information about the axial periodicity of the phase.

A remarkable feature of the results in Figs. 1(a) and 1(c) is the large separation between the peaks, corresponding to a vortex-pair width of 2.85. The mean vortex-pair width  $2L/p$  for the entire column is only 2.34. We used data similar to those in Fig. 1 to measure the local vortex-pair width as a function of  $l$ . The results are shown in Fig. 2. Near the ends of the column, where the wavy mode amplitude is small, visual measurements were also possible and are shown in the figure. It is clear that the width of the vortex pairs is dramatically increased beyond the mean value near the center of the system and decreased near the ends of the system. Similar measurements above but *near*  $R_w$  show the vortex pair widths to be very uniform. We also found during these measurements that the subharmonic exists only in the center portion of the column where the vortex pair width is larger than about 2.5.

In order to learn more about the symmetry of

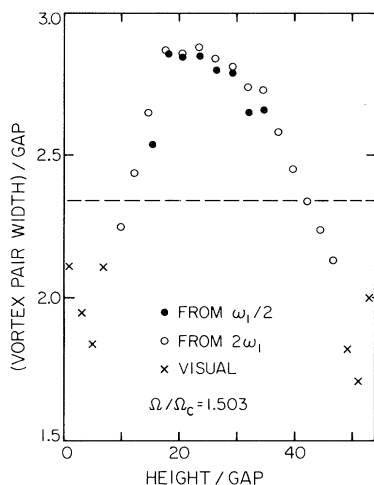


FIG. 2. The time-averaged vortex-pair width, as a function of distance above the bottom end of the column.

the subharmonic, measurements of the phase difference  $\varphi(\omega_1/2, l, \theta)$  of the spectral component at  $\omega_1/2$  were made by taking simultaneous time series at two locations. The reference location was fixed at  $l = 22.25$ , and its angular position was used as an origin to describe the azimuthal angle  $\theta$  (in the direction of rotation of the inner cylinder) between the two probes. The second probe was moved in the axial direction in steps  $\Delta l \approx 0.1$ . For  $\theta = 4.51$  rad, the phase difference  $\varphi(\omega_1/2, l, 4.51)$  (modulo  $2\pi$ ) is shown in Fig. 3 as a function of  $l$ . Although the *power* at  $\omega_1/2$  had the axial periodicity of the vortex pairs (see Fig. 1), we see that the *phase* of the subharmonic on successive vortex pairs differs by  $\pi$ . Thus, the width of the subharmonic in the axial direction is *twice* the vortex-pair width and about equal to 5.7. Similar results for  $\omega_1$  show that the phase of  $\omega_1$  repeats in the axial direction over a length equal to a *single* vortex-pair width of 2.85. Visual observations near  $\theta = \pi/2$  showed that the subharmonic corresponds to a disturbance of every other wave in both the axial and azimuthal direction, i.e., in a checkerboard pattern.

Many scans in the axial direction at various  $\theta$  yielded the phase difference at constant  $l$  as a function of  $\theta$ . Except possibly for an  $l$ -dependent additive constant, we expect  $\varphi = m\theta$ . Results for  $\varphi(\omega_1, l = 23.2, \theta)$  are shown as solid circles in Fig. 4(a). The open circles are for  $\varphi(\omega_1, l = 26.05, \theta)$  corresponding to an axial displacement by a single vortex-pair width of 2.85. The agreement between the two sets of data verifies that the mode of frequency  $\omega_1$  has the same axial width as the

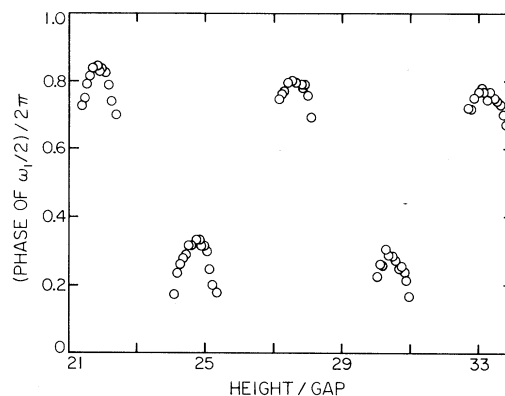


FIG. 3. The phase of the subharmonic, relative to a stationary reference signal at  $l = 22.25$ , as a function of  $l$  (height/gap). The phase shift by  $\pi$  on successive vortex pairs is evident.

vortex pairs. The solid lines are drawn with slope 3, and their agreement with the data demonstrates that  $\omega_1$  does indeed correspond to  $m = 3$ . Similar data for  $\varphi(\omega_1/2, l, \theta)$  are shown in Fig. 4(b). In that case, the solid circles are for  $\varphi(\omega_1/2, 22.25, \theta)$ , whereas open circles correspond to  $\varphi(\omega_1/2, 25.35, \theta) - \pi$ . The agreement between the open and solid circles demonstrates further the phase difference of  $\pi$  for this mode on successive

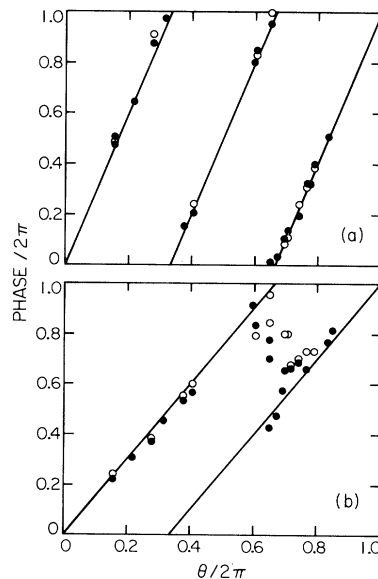


FIG. 4. The phase of (a) the  $m = 3$  mode at frequency  $\omega_1$  and (b) the subharmonic at frequency  $\omega_1/2$ , relative to a stationary reference signal at  $l = 22.25$ , as a function of the azimuthal angle  $\theta$  between the probes. (a) Solid circles are for  $l = 23.2$ , and open circles for  $l = 26.05$ . (b) Solid circles are for  $l = 22.5$ , and open circles are  $\varphi(\omega_1/2) - \pi$  for  $l = 25.35$ .

vortex pairs. The solid lines in Fig. 4(b) are drawn with slope  $\frac{3}{2}$ . Over a wide range of  $\theta$ , the data agree with the lines, indicating that over that angular range the mode indeed corresponds to  $m = \frac{3}{2}$ . There it has a wavelength equal to  $\frac{2}{3}$  the circumference, and it moves at the same speed as the  $m = 3$  mode. For  $0.6 \leq \theta/2\pi \leq 0.7$ , the mode develops a phase anomaly and “drops back” by half a wavelength so as to be able to continue periodically around the annulus. At slightly different axial positions on the same vortex pair, we have observed the transition taking place in the range  $0.5 \leq \theta/2\pi \leq 0.8$  by “jumping ahead” by half a wavelength. This transition region is stationary in the laboratory frame, possibly because of pinning by slight geometric imperfections.

We are grateful to R. J. Donnelly, K. Park, E. D. Siggia, and H. L. Swinney for helpful discussions. This work was supported in part by National Science Foundation Grant No. DMR79-23289, and by the Consejo Nacional de Ciencia Tecnología de México and the Escuela Superior

de Física y Matemática, Comisión para el Fomento Académico y Administrativo, Instituto Politécnico Nacional, Mexico.

<sup>1</sup>D. Coles, *J. Fluid Mech.* **21**, 385 (1965).

<sup>2</sup>M. Gorman, H. L. Swinney, and D. A. Rand, *Phys. Rev. Lett.* **46**, 992 (1981).

<sup>3</sup>D. A. Rand, to be published.

<sup>4</sup>See, for instance, T. B. Benjamin and T. Mullin, *Proc. Roy. Soc. London, Ser. A* **377**, 221 (1981).

<sup>5</sup>For a recent review, see R. C. DiPrima and H. L. Swinney, in *Hydrodynamic Instabilities and the Transition to Turbulence*, edited by H. L. Swinney and J. P. Gollub (Springer, Berlin, 1981).

<sup>6</sup>As discussed below, WVF results in a local increase of  $\lambda$  near the center and a local decrease of  $\lambda$  near the ends of the column. When the local  $\lambda$  is greater than the maximum or less than the minimum  $\lambda$  which is stable for TVF at a given  $R/R_c$ , a transition to a different value of  $p$  occurs.

<sup>7</sup> $\varphi(\omega) = -\tan^{-1}[(R_2 I_1 - R_1 I_2)/(R_1 R_2 + I_1 I_2)]$ , where  $R_i(\omega)$  and  $I_i(\omega)$  are the real and imaginary parts of the Fourier transforms of the two signals  $i = 1, 2$ .

## Stimulated Raman Backscatter from a Magnetically Confined Plasma Column

A. A. Offenberger, R. Fedosejevs, W. Tighe, and W. Rozmus<sup>(a)</sup>

*Department of Electrical Engineering, University of Alberta, Edmonton, Alberta T6G 2G7, Canada*

(Received 28 December 1981)

Stimulated Raman backscatter from long-scale-length, magnetically confined, underdense plasma has been studied for incident CO<sub>2</sub> laser intensities up to  $2.5 \times 10^{11}$  W/cm<sup>2</sup>. Above an incident threshold of  $4 \times 10^{10}$  W/cm<sup>2</sup> the reflectivity rapidly rises to a saturated value of 0.7%. The measurements are in good agreement with a theoretical model of absolute instability which includes both collisional and Landau damping due to hot-electron production.

PACS numbers: 52.25.Ps, 52.55.Ke

Parametric instabilities in plasmas have recently been the subject of intense theoretical investigation<sup>1-9</sup> because of their possible effect in reducing absorption and producing superthermal particles<sup>10</sup> in laser-driven fusion. Stimulated Raman scattering (SRS), which involves the scattering of an electromagnetic wave from an enhanced electron plasma wave, is one such instability. Unlike stimulated Brillouin scattering (SBS), which involves an ion wave with little dispersion and therefore satisfies easy matching conditions, SRS requires a long-scale-length underdense plasma ( $n < n_c/4$ ) in order to provide

phase matching and growth for the highly dispersive electron wave. As a consequence, SRS has not been extensively studied in present-day laser-target interaction experiments in which density-gradient scale lengths,  $L_n$ , are short. For future reactor-size plasmas, however, long gradient scale lengths are expected.

A linear magnetically confined plasma, on the other hand, does offer the prospect for providing large  $L_n$  and, indeed, was used in an early experimental study<sup>11</sup>—wherein SRS reflectivity levels of  $10^{-5}$  were reported. In the present study, we report spectrally and temporally resolved meas-